Circuit Model for Lamellar Metallic Gratings in the Sub-wavelength Regime

Amin Khavasi and Khashayar Mehrany

***Abstract*—A circuit model is proposed for periodic one-dimensional array of metallic strips in the sub-wavelength regime. The parameters of the proposed circuit and their dependence on frequency are all explicitly given by closed form expressions. The necessity of using numerical simulation to extract model parameters is thus sidestepped. It is demonstrated that the proposed model is valid at different incident angles and for arbitrary surrounding mediums given that there is only one propagating diffracted order outside the grating and only one guided mode supported by the slits. Both major polarizations are studied in this paper.**

***Index Terms*— metallic grating, sub-wavelength structures, circuit model**

I. Introduction

RECENT researches revealed that metallic structures with sub-wavelength features have a great potential for producing unusual electromagnetic responses [1-4]. Creation of high-impedance surfaces [5], effective plasmonic behavior [6], high index of refraction [3] and negative refractive index [7] are some of these interesting examples. In particular, extra-ordinary transmission (EOT) through sub-wavelength periodic array of holes or slits perforated in relatively thick metals has caused intensive research efforts since its discovery by Ebbesen et. al. [8]. Many authors have attributed this phenomenon to the excitation of surface plasmon polaritons on the periodically structured surface of the metal screen [9]-[11] but some has also tried to ascribe this phenomenon to the resonance of TEM modes supported by the metallic slits present in the structure[12].

Equivalent circuit models are recently proposed for these structures and the EOT in the sub-wavelength regime is thus explained by using the impedance matching concept. Such circuit models have been thus far developed for two-dimensional array of holes [13] and for one-dimensional array of metallic slits [14]. The structure in the latter case has been modeled for TM polarization by using two capacitors to account for the evanescent fields on the surfaces of the structure and a transmission line to account for the TEM mode propagating inside the slits. This model, however, has some limitations. First, the capacitances of the model capacitors and their frequency dependence are not explicitly given in closed form expressions and have to be derived numerically, e.g. by mode matching [14]. Second, the proposed model is limited to normal incidence and should be modified for arbitrary angle of incidence. Although it is straightforward to generalize the model for TM waves at arbitrary angle of incidence, accurate modeling of TE waves is more delicate. Third, outside the grating region is assumed to be free space and thus the model should be generalized to consider any homogeneous structure with arbitrary refractive index. This latter limitation is however partially overcome in [15], where the full wave analysis of the structure is to be carried out at a few specific frequencies to extract circuit parameters for TM polarized waves.

The abovementioned limitations are addressed in this paper, where a one-dimensional array of metallic strips sandwiched between arbitrary homogeneous media is considered for oblique incidence at both major polarizations. Parameters of the appropriate circuit model are all given by closed form expressions to avoid resorting to additional numerical efforts for their extraction. First, the TM polarization is studied and then the Babinet principle is applied to modify the model for TE polarization. It is shown that the capacitors in the TM circuit model should be replaced with inductors and that the transmission line accounting for the grating region should be related to the characteristic impedance and propagation constant of the first TE mode propagating between the slits.

The paper is organized as follows: Section II is devoted to the detailed description of the proposed circuit model, whose limitations are expounded in detail in the next section. Numerical results are then given in section IV, where the accuracy of the proposed model is compared against numerical results obtained by using a rigorous approach. Finally, the conclusions are made in section V.

II. The Proposed Circuit Model

The geometry of the structure to be studied is shown in Fig. 1. The periodic arrangement of metallic strips in a medium with refractive index of n_2, forms a grating with period d and thickness h. The spacing between metal strips is w and the grating region is sandwiched between two homogenous regions with refractive indices of n_1 and n_3. The magnetic permeability is everywhere equal to that of the free space. The structure is illuminated by a uniform plane wave whose wave vector is incident at angle θ with respect to the Oz axis. The free space wavelength of the wave is denoted by λ.

Similar to the proposed model in [14], the grating region is modeled by a transmission line, which is terminated by reactive components to account for the evanescent waves storing electromagnetic energy at the vicinity of the external

Manuscript received ???

The authors are with Electrical Engineering Department, Sharif University of Technology, Tehran 11155-4363, Iran (e-mail: mehrany@sharif.edu).

interfaces of the grating. First, the TM polarization is investigated and then some necessary changes are made to consider the TE polarization.

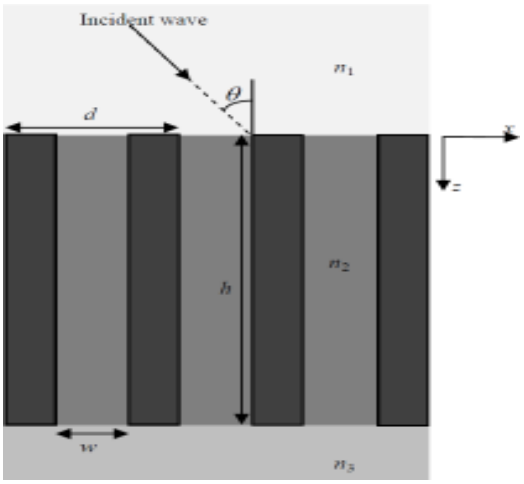

Fig. 1. The geometry of the structure under study: periodic array of metallic strips under the incidence of a uniform plane wave.

A. TM polarization

The schematic of the proposed model for TM polarized waves is shown in Fig. 2 and is similar to the proposed model in [14]. The transmission line models the field behavior as it travels between the slits. It is geometrically obvious that the length of this transmission line should be h and its propagation constant; β_2^{TM}, and characteristic impedance; Z_2^{TM}, should be equal to those of the TEM mode supported by a parallel plate waveguide whose plates are separated by a distance w [14]:

$$\beta_2^{TM} = k_0 n_2 \tag{1}$$

$$Z_2^{TM} = \frac{\eta_0 w}{n_2 d} \tag{2}$$

where $k_0 = 2\pi/\lambda$ and $\eta_0 \approx 120\pi$ are the free space wave number and impedance, respectively.

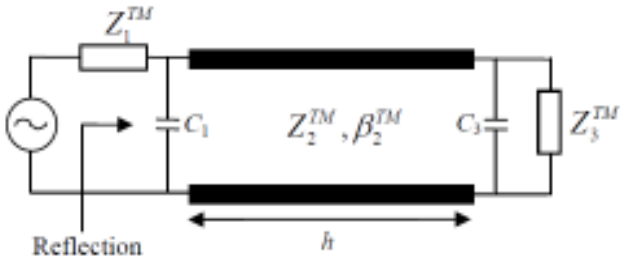

Fig. 2. The proposed circuit to model the structure shown in Fig. 1 for TM polarized incident waves.

The transmission line is terminated by Z_1^{TM}, C_1 and Z_3^{TM}, C_3 at its input and output terminals; respectively. The Z_1^{TM} and Z_3^{TM} impedances represent electromagnetic wave impedances in the incident and transmission homogenous regions having refractive indices of n_1 and n_3; respectively. It is therefore straightforward to show that

$$Z_i^{TM} = \eta_0 \cos\theta_i / n_i, \ i = 1,3 \tag{3}$$

where θ_1 and θ_3 are the zeroth diffracted order angles in regions 1 and 3, respectively. It is worth noting that $\theta_1 = \theta$.

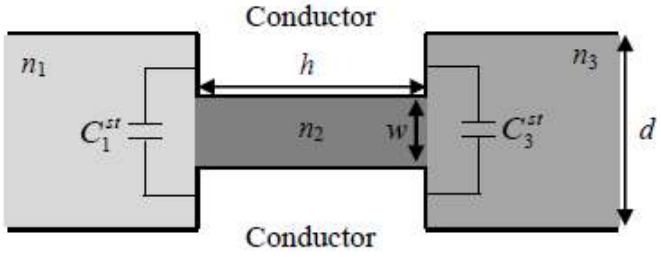

Fig. 3. The electrostatic problem that can be solved to determine the static values of the capacitors C_1 and C_3 in the proposed model shown in Fig. 2.

The capacitors C_1 and C_3 account for the evanescent fields and are wavelength-dependent. It is however already shown that these capacitors are at large enough wavelengths equal to the edge capacitances C_1^{st} and C_3^{st} that are schematically depicted between the metallic sidewalls shown in Fig. 3 [14]. It is for this reason possible to obtain the static values of the sought-after capacitances $C_1 = C_1^{st}$ and $C_3 = C_3^{st}$ by finding the edge capacitances in Fig. 3. The following formula is already derived for the static capacitors for $n_1 = n_3 = 1$ [16]:

$$C_1^{st} = C_3^{st} = C_0^{st} \cong \frac{d \ \mathrm{Ln}\left(\csc\left(\frac{\pi w}{2d}\right)\right)}{\eta_0 c_0 \pi} \tag{4}$$

Here, c_0 denotes the speed of light in free space. This expression is extended here to consider arbitrary n_1 and n_3:

$$C_i^{st} \cong n_i^2 C_0^{st}, \ i = 1,3 \tag{5}$$

The details of this extension are presented in the appendix.

The wavelength dependence of C_1 and that of C_3 can then be determined by using the following expression, which is based on the frequency dependence of the wave impedance of TM modes in parallel plate waveguides [14]:

$$C_i \cong C_i^{st}\left[1 - \alpha + \frac{\alpha}{\sqrt{1-(\lambda_C/\lambda)^2}}\right], \ i = 1,3 \tag{6}$$

Here, $\lambda_C = n_i(1+\sin\theta_i)d$ is the wavelength at which the minus-first diffracted order becomes propagating and α is an unknown coefficient left to be determined. As expected, C_i^{st} is the limit point of the above expression when the wavelength approaches infinity, i.e. $\lambda \to \infty$. This expression is already reported in [14] but the fitting α to yield the correct values of the capacitors at different wavelengths was left to be obtained by the mode-matching technique or similar rigorous approaches. In the present study, we found that $\alpha = (1 - f^4)^{1/2}$; where $f = 1 - w/d$ stands for the fill factor of the grating, is an accurate enough approximation that provides very good results.

As a naïve approximation for small fill factors, the expression in (6) can be further approximated by using $\alpha = 1$:

$$C_i \cong \frac{C_i^{st}}{\sqrt{1-\left(\frac{\lambda_C}{\lambda}\right)^2}},\ i=1,3 \tag{7}$$

B. TE polarization

It is a well-known fact that the Babinet's principle can be applied to modify the proposed model for TE polarization when the grating thickness is $h = 0$ [16]. Since the transmission line is for $h = 0$ eliminated from the model, the only remaining modification will be replacing the shunt capacitors in Fig. 2 with shunt inductors whose value is to be determined shortly. Given that the capacitors C_1 and C_3 of the proposed circuit to model the structure for TM polarization are connected in parallel whenever $h = 0$, the TM surface impedance of the complement of the structure with $h = 0$ and $n_1 = n_3 = 1$ reads as:

$$Z_S^{TM} = -j/(2\omega C) \tag{8}$$

where $C = C_1 = C_3$. It should be noted that the width of the metal strips in the complement of the structure is $d–w$. It is for this reason that $\alpha^c = (1 - (w/d)^4)^{1/2}$, and w in (4) is replaced by $d–w$ in (11).

As maintained by the Babinet's principle; now, the surface impedance of the original structure for TE polarization with $h = 0$ reads as [16]:

$$Z_{S'}^{TE} = \eta_0^2/\left(4Z_S^{TM}\right) \tag{9}$$

which can be further simplified to

$$Z_{S'}^{TE} = j\omega L/2 \tag{10}$$

where $L = C\eta_0^2$. It is thus formed by two inductors L_1 and L_3=L_1 connected in parallel and we have:

$$L_i \cong \frac{\eta_0 d\ \mathrm{Ln}\left(\csc\left(\frac{\pi(d-w)}{2d}\right)\right)}{c_0\pi\sqrt{1-\left(\frac{\lambda_C}{\lambda}\right)^2}},\ i=1,3 \tag{11}$$

It is worth noting that we had set $n_1 = n_3 = 1$ in the complement of the structure to ensure that the inductors in the original structure for the TE polarization are calculated under the assumption that the magnetic permeability is everywhere equal to that of the free space. That is why L_3=L_1 does not depend on the refractive index of the dielectric regions n_1 and n_3.

Since these shunt inductors represent only evanescent fields at the upper and lower interfaces of the grating; however, the electromagnetic behavior of waves propagating within the grating region remains to be taken into account. A transmission line is for this reason employed to complete the proposed model for the general case when the grating thickness is not necessarily zero. The schematic of the proposed model is shown in Fig. 4. Once again, it is geometrically obvious that the length of this transmission line should be h and its propagation constant; β_2^{TE}, and characteristic impedance; Z_2^{TE}, should be related to the first TE mode supported by the same parallel plate waveguide whose plates are separated by a distance w:

$$\beta_2^{TE} = \sqrt{k_0^2 n_2^2 - \left(\frac{\pi}{w}\right)^2} \tag{12}$$

$$Z_2^{TE} = \eta_0\left(\frac{w}{d}\right)\frac{k_0}{\beta_2^{TE}} \tag{13}$$

It should be however noticed that using the electromagnetic characteristics of the first TE mode in the transmission line of the model instead of the electromagnetic characteristics of the TEM mode has some implications. The transverse electromagnetic field profile of the first TE mode is sinusoidal and not uniform:

$$E_y = E_0 \sin\left(\frac{\pi x}{w}\right)e^{-j\beta_2^{TE}z} \tag{14}$$

$$H_x = H_0 \sin\left(\frac{\pi x}{w}\right)e^{-j\beta_2^{TE}z} \tag{15}$$

The electric voltage observed between the two plates is then related to the electric field amplitude; E_0, as follows:

$$V = \int_0^w E_0 \sin\left(\frac{\pi x}{w}\right)e^{-j\beta_2^{TE}z}dx = \frac{2w}{\pi}E_0 \tag{16}$$

Furthermore, the power flow of the TE mode along the waveguide is on the one hand:

$$P = \frac{1}{2}\int_0^w E_y\overline{H_x}dx = \frac{wE_0\overline{H_0}}{4} \tag{17}$$

where $\overline{H_0}$ and $\overline{H_x}$ denote the conjugate of H_0 and H_x, respectively. The power flow in terms of electric voltage and current is on the other hand

$$P = \frac{V\bar{I}}{2} \tag{18}$$

where $\bar{I}$ denotes the conjugate of I, the electric current.

It is thus straightforward to relate the electric current; I, to the magnetic field amplitude; H_0, by combining equations (16), (17) and (18): $I = \pi H_0/4$.

The circuit impedance V/I is then not equal to the wave impedance E_0/H_0 and we have:

$$\frac{V}{I} = \frac{8}{\pi^2}\frac{E_0}{H_0} \tag{19}$$

It is for this reason necessary to insert a transformer with $n^2 = \pi^2/8$ to duly transform the wave impedance into electric impedance in the circuit model shown in Fig. 4.

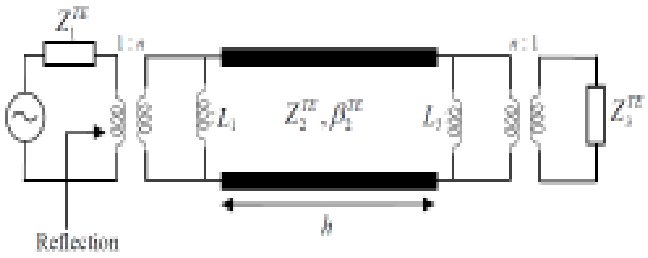

Fig. 4. The proposed circuit to model the structure shown in Fig. 1 for TE polarized incident waves.

Since the electric current and voltage in the homogenous regions outside the grating are directly proportional to the electric and magnetic field amplitudes, the Z_1^{TE} and Z_3^{TE} impedances in the model still represent the electromagnetic wave impedances in the incident and transmission homogenous regions having refractive indices of n_1 and n_3; respectively:

$$Z_i^{TE} = \eta_0 / (n_i \cos\theta_i), \quad i = 1, 3 \tag{20}$$

III. Limitations of The Model

It is obvious that the accuracy of the proposed circuit model is limited to the frequency range where there is only one propagating mode inside the slits and only one diffracted order outside the grating.

The condition of having only one propagating mode between the slits requires

$$\lambda > w n_2 / 2 \tag{21}$$

for the TM polarization and

$$\lambda > w n_2 \tag{22}$$

for the TE polarizations. In these expressions, $wn_2/2$ and wn_2 are cutoff wavelengths of the TM_1 and TE_2 modes of the slits, respectively.

The condition of having only one propagating diffracted order requires:

$$\lambda > (n_{\max} + n_1 \sin\theta) d \tag{23}$$

where n_{max} = max{n_1, n_3}. In this fashion, even the smallest Floquet wave vector corresponds to evanescent Floquet orders in the incident and transmission regions.

IV. Numerical Example

The usefulness of the proposed model is demonstrated through some numerical examples. The first example is a grating whose parameters in accordance with Fig. 1 are as follows: n_1 = 1.4, n_2 = 1, n_3 = 1.2, w = 0.2 cm, h = 3d = 3 cm. The incident wave is a TM polarized plane wave. The power transmission of this structure is plotted in Fig. 5 versus the normalized frequency $\omega_n = d/\lambda$ at normal incidence. The results are obtained by using the proposed transmission line model (dotted line) and the rigorous approach of [17] (solid line) The MATLAB code for this method is now available at http://ee.sharif.edu/~khavasi/index_files/ASR.zip. We marked the maximum frequency limit in which the proposed model is valid with a straight dashed line. This restriction is imposed by (23). For frequencies within this limit, the proposed approximate model virtually coincides with the rigorous model.

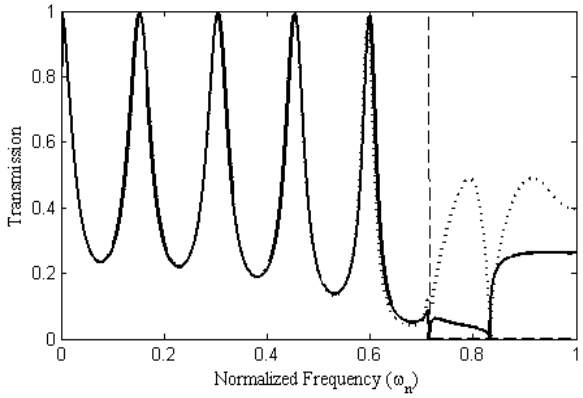

Fig. 5. Transmitted power through a grating illuminated by a TM polarized incident plane wave versus normalized frequency calculated by the proposed model (dotted line) and the rigorous approach of [17] (solid line). The grating parameters are: n_1 = 1.4, n_2 = 1, n_3 = 1.2, w = 0.2 cm and h = 3d = 3 cm. The grating is under normal incidence. The straight dashed lines in this figure represent the maximum frequency limit obtained by imposing (23).

The performance of the TM model is also verified for different incident angles and different slit widths. The transmitted power in the previous example is once again plotted versus the incident angle and versus the normalized slit width w/d in Figs. 6, and 7, respectively. The normalized frequency in these figures is ω_n = 0.34. The results obtained by using the proposed TM model (dotted line) is compared against those obtained by using the rigorous approach of [17] (solid line).

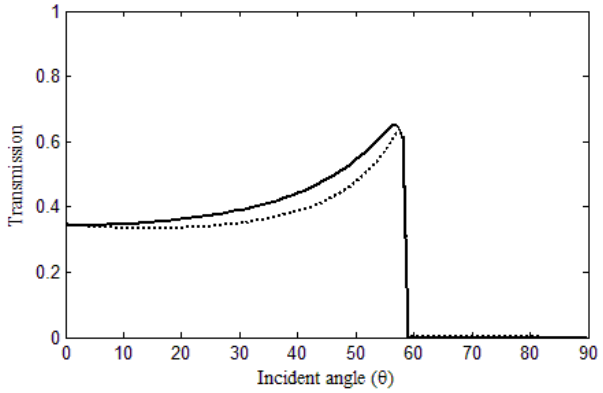

Fig 6. Transmitted power through a grating illuminated by a TM polarized incident plane wave versus the incident angle calculated by the proposed model (dotted line) and the rigorous approach of [17] (solid line). The grating parameters are: n_1 = 1.4, n_2 = 1, n_3 = 1.2, w = 0.2 cm and h = 3d = 3 cm. The normalized frequency is ω_n = 0.34.

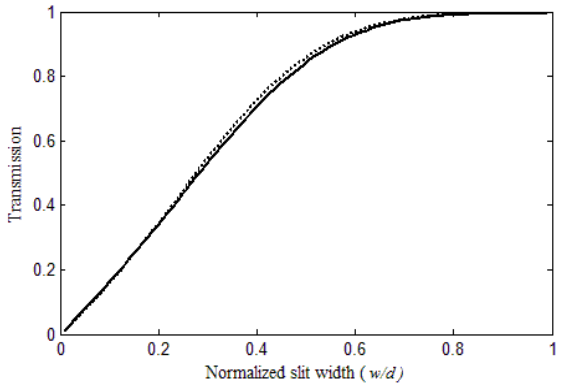

Fig 7. Transmitted power through a grating illuminated by a TM polarized incident plane wave versus the normalized slit width calculated by the proposed model (dotted line) and the rigorous approach of [17] (solid line). The grating parameters are: $n_1 = 1.4$, $n_2 = 1$, $n_3 = 1.2$ and $h = 3d = 3$ cm. The grating is under normal incidence and the normalized frequency is $\omega_n = 0.34$.

The next example is an array of metallic strips illuminated by a TE polarized wave. The spacing between the strips is $w = 0.8$ cm. The other parameters are: $n_1 = 1.2$, $n_2 = 2$, $n_3 = 1$, $h = 3$ cm, and $d = 1$ cm. The transmitted power of the structure is shown in Fig. 8 versus normalized frequency for $\theta = 0°$. Similarly, the results are obtained by two approaches: the proposed TE model (dotted line) and the rigorous approach of [17] (solid line). The maximum frequency limits imposed by (22) and (23) are marked in Fig. 8 by straight solid and dashed lines, respectively. As expected, the transmission line model is very accurate below the frequency range given in (22) and (23). It is however interesting that even for the normalized frequencies larger than the upper-limit imposed by (22), the proposed model is still working. This can be explained by pointing out that the higher order modes in the parallel plate waveguide formed by the metallic strips are not excited at normal incidence.

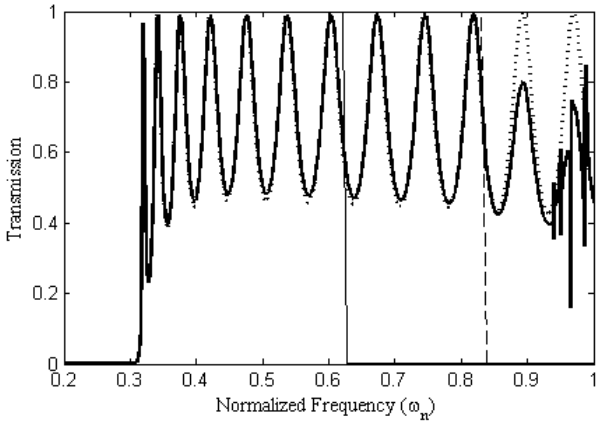

Fig. 8. Transmitted power through a grating illuminated by a TE polarized incident plane wave versus normalized frequency calculated by the proposed model (dotted line) and the rigorous approach of [17] (solid line). The grating parameters are: $n_1 = 1.2$, $n_2 = 2$, $n_3 = 1$, $w = 0.8$ cm and $h = 3d = 3$ cm. The grating is under normal incidence. The straight solid and dashed lines in this figure represent the maximum frequency limit obtained by imposing (22) and (23), respectively.

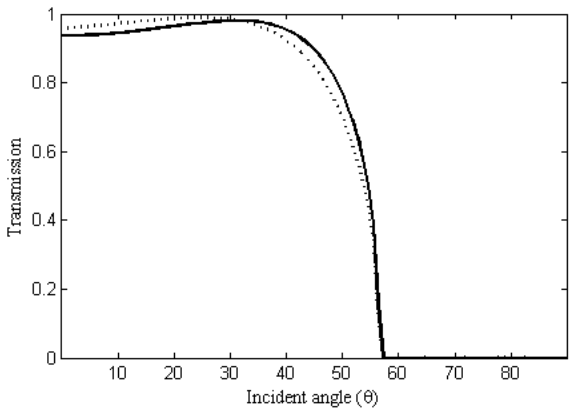

Fig 9. Transmitted power through a grating illuminated by a TE polarized incident plane wave versus incident angle calculated by the proposed model (dotted line) and the rigorous approach of [17] (solid line). The grating parameters are: $n_1 = 1.2$, $n_2 = 2$, $n_3 = 1$, $w = 0.8$ cm and $h = 3d = 3$ cm. The normalized frequency is $\omega_n = 0.34$.

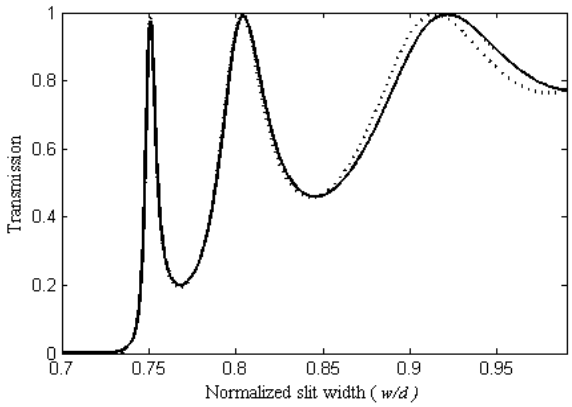

Fig 10. Transmitted power through a grating illuminated by a TE polarized incident plane wave versus normalized slits' width calculated by the proposed model (dotted line) and the rigorous approach of [17] (solid line). The grating parameters are: $n_1 = 1.2$, $n_2 = 2$, $n_3 = 1$ and $h = 3d = 3$ cm. The grating is under normal incidence and the normalized frequency is $\omega_n = 0.34$.

The performance of the TE model is similarly tested at different incident angles and for different slit widths. The transmitted power of the same grating studied in the previous example is plotted versus the incident angle and versus the slit width in Figs. 9, and 10, respectively. The normalized frequency is $\omega_n = 0.34$ in these figures. Once more, the results obtained by using the proposed TE model (dotted line) is compared against those obtained by using the rigorous approach of [17] (solid line) and an excellent agreement is observed.

V. Conclusion

An equivalent circuit has been proposed for modeling one-dimensional metallic gratings in the sub-wavelength regime for both major polarizations. The proposed model for the TM polarization is composed of a transmission line for the slits and two capacitors for the evanescent fields in the upper and lower regions at the vicinity of the grating surface. The capacitance of the model capacitors has been given in a simple closed form expression in terms of the free space wavelength, the incident

angle, the slits' width and the refractive index of incident and transmission regions. By applying the Babinet's principle and using electromagnetic characteristics of TE_1 mode, the proposed model is revised for TE waves.

It has been demonstrated that the equivalent circuits render accurate results when there is only one propagating mode supported by the slits formed between the metallic strips and when the zeroth diffracted order is the only propagating order in homogenous regions outside the grating region.

The results of the proposed equivalent circuit are compared with those obtained by following a rigorous method in a typical numerical example. An excellent agreement is observed between the two methods.

APPENDIX

Since the static edge capacitances C_1^{st} and C_3^{st} in Fig. 3 are already determined for $n_1 = n_3 = 1$, it is not necessary to re-solve the Laplace equation and apply the new boundary conditions to obtain C_1^{st} and C_3^{st} for arbitrary n_1 and n_3. This is due to the fact that the Laplace equation; $\nabla^2 V = 0$, governing the electrostatic potential and its corresponding electric field ; $E = -\nabla V$, are both independent of n_1 and n_3. Neglecting the normal component of the electric field at the interface between the dielectric regions n_1, n_2, and n_3, n_2, the appropriate boundary conditions, i.e. the continuity of the tangential electric field, are also independent of n_1 and n_3. Therefore, the electrostatic potential V and its corresponding electric field E remain unchanged when regions 1 and 3 are not unity anymore. The accumulated surface charge densities on the upper and lower metallic plates of the edge capacitances C_1^{st} and C_3^{st} are on the other hand proportional to the n_1^2 and n_3^2, respectively. This is due to the fact that while the normal component of the electric field at the interface between the dielectric region and metallic plates is unchanged, the permittivity of the dielectric region is now either n_1^2 or n_3^2 and we know that the surface charge density is equal to the multiplication of the normal component of the electric field and the permittivity of the dielectric region, i.e. $\rho_s = \varepsilon E_n$. The total charge accumulated on the edge capacitance C_i^{st} is therefore $Q_i = n_i^2 Q_0$, where $i = 1,3$ and Q_0 indicates the accumulated electric charge on the edge capacitance C_0^{st} when $n_1 = n_3 = 1$. The sought-after static edge capacitance C_i^{st} can then be written down as:

$$C_i^{st} = \frac{Q_i}{\Delta V} = \frac{n_i^2 Q_0}{\Delta V} = n_i^2 C^{st}, \quad i = 1,3 \qquad \text{(A.1)}$$

where ΔV is the potential difference between the two plates. As already mentioned, the electrostatic potential and consequently ΔV are independent of n_1 and n_3.

ACKNOWLEDGMENT

This work was supported by the Iran Telecommunication Research Center.

REFERENCES

[1] J. B. Pendry, A. J. Holden, D. J. Robbins, and W. J.Stewart, "Magnetism from conductors and enhanced non-linear phenomena" *IEEE Trans. Microwave Theory Tech.* vol. 47, no. 11, pp. 2075-2084, Nov. 1999.

[2] D. R. Smith and N. Kroll, "Negative refractive index in left-handed materials," *Phys. Rev. Lett.* vol. 85, no. 14, pp. 2933-2936, Oct. 2000.

[3] J. T. Shen, P. B. Catrysse and S. Fan, "Mechanism for Designing Metallic Metamaterials with a High Index of Refraction," *Phys. Rev. Lett.,* vol. 94, no. 19 , pp. 197401-4, May 2005.

[4] J. B. Pendry, L. Martı´n-Moreno, and F. J. Garcıa-Vidal, "Mimicking surface plasmons with structured surfaces," *Science,* vol. 305, pp. 847, Aug. 2004.

[5] D. Sievenpiper, L. Zhang, R. F. Jimenez Broas, N. G. Alexopolous, and E. Yablonovitch, "High-impedance electromagnetic surfaces with a forbidden frequency band", *IEEE Trans. Microwave Theory Tech.*, vol. 47, no. 11, pp. 2059-2074, Nov. 1999.

[6] J. B. Pendry, A. J. Holden, W. J. Stewart, and I. Youngs, "Extremely low frequency plasmons in metallic mesostructures," *Phys. Rev. Lett.*, vol. 76, no. 25, pp. 4773–4776, Jun. 1996.

[7] D. R. Smith,W. J. Padilla, D. C. Vier, S. C. Nemat-Nasser, and S. Schultz, "Composite medium with simultaneously negative permeability and permittivity," *Phys. Rev. Lett.*, vol. 84, no. 18, pp. 4184–4187, May 2000.

[8] T. W. Ebbesen, H. J. Lezec, H. F. Ghaemi, T. Thio, and P. A. Wolff, "Extraordinary optical transmission through sub-wavelength hole arrays," *Nature*, vol. 391, pp. 667–669, Feb. 1998.

[9] R. Sambles, "More than transparent," *Nature*, vol. 391, pp. 641–642, Feb. 1998.

[10] H. F. Ghaemi, T. Thio, D. E. Grupp, T. W. Ebbesen, and H. J. Lezec, "Surface plasmons enhance optical transmission through subwavelength holes," *Phys. Rev. B, Condens. Matter*, vol. 58, no. 15, pp. 6779–6782, Sep. 1998.

[11] D. E. Grupp, H. J. Lezec, T. W. Ebbesen, K. M. Pellerin, and T. Thio, "Crucial role of metal surface in enhanced transmission through subwavelength apertures," *Appl. Phys. Lett.*, vol. 77, no.11, pp. 1569–1571, Sep. 2000.

[12] J. A. Porto, F. J. García-Vidal, and J. B. Pendry, "Transmission resonances on metallic gratings with very narrow slits," *Phys. Rev. Lett.*, vol. 83, no. 14, pp. 2845–2848, Oct. 1999.

[13] F. Medina, F. Mesa, and R. Marqués, "Extraordinary transmission through arrays of electrically small holes from a circuit theory perspective," *IEEE Trans. Microw. Theory Tech.*, vol. 56, no. 12, pp. 3108–3120, Dec. 2008.

[14] F. Medina, F. Mesa, and D. C. Skigin, "Extraordinary transmission through arrays of slits: a circuit theory model," *IEEE Trans. Microw. Theory Tech.*, vol. 58, no. 1, pp. 105–115, Jan. 2010.

[15] R. Rodriguez-Berral, F. Mesa, and F. Medina, "Circuit model for a periodic array of slits sandwiched between two dielectric slabs," *Appl. Phys. Lett.*, vol. 96, no. 16, pp. 1104(3), 2010.

[16] O. Luukkonen, C. Simovski, G. Granet, G. Goussetis, D. Lioubtchenko, A. V. Räisänen, and S. A. Tretyakov, "Simple and analytical model of planar grids and high-impedance surfaces comprising metal strips or patches," *IEEE Trans. Antennas Propag.*, vol. 56, no. 6, June 2008.

[17] A. Khavasi and K. Mehrany, "Adaptive Spatial Resolution in Fast, Efficient, and Stable Analysis of Metallic Lamellar Gratings at Microwave Frequencies," IEEE Trans. Antennas Propag., vol. 57, no.4, pp. 1115-1121, Apr. 2009.

Amin Khavasi was born in Zanjan, Iran, on January 22, 1984. He received the B.Sc., and M.Sc. degrees from Sharif University of Technology, Tehran, Iran, in 2006, and 2008, respectively, all in electrical engineering. He is currently working toward the Ph.D. degree at the Sharif University of Technology.

His research interest include photonics, circuit modeling of photonic structures and computational electromagnetic.

Khashayar Mehrany was born in Tehran, Iran, on September 16, 1977. He received the B.Sc., M.Sc., and Ph.D. (*magna cum laude*) degrees from Sharif University of Technology, Tehran, Iran, in 1999, 2001, and 2005, respectively, all in electrical engineering.

Since then, he has been an Associate Professor with the Department of Electrical Engineering, Sharif University of Technology. His research interests include photonics, semiconductor physics, nanoelectronics, and numerical treatment of electromagnetic problems.